Zwitter-Wettability and Antifogging Coatings with Frost-Resisting Capabilities

Hyomin Lee,[†] Maria L. Alcaraz,[†] Michael F. Rubner,[‡,*] and Robert E. Cohen[†,*]

[†]Department of Chemical Engineering, Massachusetts Institute of Technology, Cambridge, Massachusetts 02139, United States and [‡]Department of Materials Science and Engineering, Massachusetts Institute of Technology, Cambridge, Massachusetts 02139, United States

ABSTRACT Antifogging coatings with hydrophilic or even superhydrophilic wetting behavior have received significant attention due to their ability to reduce light scattering by film-like condensation. However, under aggressive fogging conditions, these surfaces may exhibit frost formation or excess and nonuniform water condensation, which results in poor optical performance of the coating. In this paper, we show that a zwitter-wettable surface, a surface that has the ability to rapidly absorb molecular water from the environment while simultaneously appearing hydrophobic when probed with water droplets, can be prepared by using hydrogen-bonding-assisted layer-by-layer (LbL) assembly of poly(vinyl alcohol) (PVA) and poly(acrylic acid) (PAA). An additional step of functionalizing the nano-blended PVA/PAA multilayer with poly(ethylene glycol methyl ether) (PEG) segments produced a significantly enhanced antifog and frost-resistant behavior. The addition of the PEG segments was needed to further increase the nonfreezing water capacity of the multilayer film. The desirable high-optical quality of these thin films arises from the nanoscale control of the macromolecular complexation process that is afforded by the LbL processing scheme. An experimental protocol that not only allows for the exploration of a variety of aggressive antifogging challenges but also enables quantitative analysis of the antifogging performance *via* real-time monitoring of transmission levels as well as image distortion is also described.

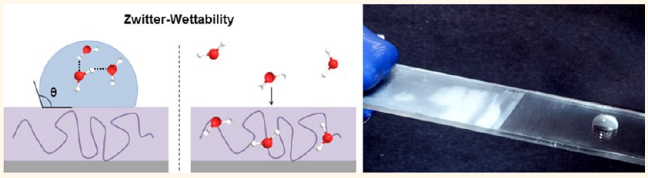

KEYWORDS: antifogging · zwitter-wettability · antifrost · layer-by-layer · wetting

Over the past decade, many research groups[1−33] have worked to develop stable, effective antifogging (AF) coatings capable of handling a wide range of environmental challenges. Although many of these AF coatings perform satisfactorily in specifically defined antifogging challenges including such tests as the Erlenmeyer steam test and the cold-fog test,[1−33] there is no single quantitative test that provides all the information needed to assess the full optical performance of the coating. For example, even coatings that maintain high levels of light transmission during an aggressive fogging challenge, under specific conditions may produce significant image distortion due to excess or nonuniform water condensation (Supporting Information Figure S1a). Thus, to truly understand the key parameters necessary for designing widely applicable antifogging coatings, it is essential to evaluate both light transmission and image distortion effects under a wide range of controlled environmental conditions.

In this work, we establish an experimental protocol that allows for the exploration of a variety of aggressive antifogging challenges by controlling not only the initial substrate temperature (T_i) but also the environmental conditions in which the AF behavior is recorded, such as temperature (T_f) and relative humidity (%RH_f). This protocol also enables quantitative analysis of the antifogging performance *via* real-time monitoring of transmission levels as well as image distortion. Although others[22,33] have attempted to quantitatively characterize antifogging performance by measuring time-dependent light transmission or haze values in accordance with ASTM standards, these methodologies may not always reveal the true optical performance of the coating.

In the process of using this new protocol to evaluate our antifog coatings, we realized that, under some extreme conditions, many coatings fail to maintain high transmission levels coupled with low image distortion values. As a result, we worked to develop a

* Address correspondence to rubner@mit.edu (M.F.R), recohen@mit.edu (R.E.C).

Received for review October 31, 2012 and accepted January 29, 2013.

Published online January 29, 2013
10.1021/nn3057966

superior antifog coating that could handle aggressive temperature/humidity conditions including those that would normally produce severe frosting on surfaces. Herein, we describe the development of a new coating system that maintains excellent optical clarity under conditions that would normally produce extreme fogging and/or frosting.

This new coating system is based on a layer-by-layer (LbL)-assembled multilayer comprised of poly(vinyl alcohol) (PVA) and poly(acrylic acid) (PAA). Previously, we have shown that hydrogen-bonded multilayer thin films consisting of PVA and PAA can be assembled under acidic conditions (pH 2.0) and further stabilized to withstand higher pH conditions by a thermal cross-linking treatment.[34] Although this multilayer coating exhibits good antifog properties, we find that an additional step of adding poly(ethylene glycol methyl ether) (PEG) segments throughout the resultant LbL-assembled multilayer film produces significantly enhanced antifog and antifrosting behavior. Antifrosting in this context refers to the ability of a coating to resist frost formation when a sample is held at very low initial substrate temperatures (T_i, where T_i is less than the freezing temperature of water) and then exposed to higher temperatures and high humidity.

In contrast to many antifogging coatings with hydrophilic[1] or even superhydrophilic[21,30] wetting behavior, PEG-functionalized PVA/PAA LbL-assembled multilayer films exhibit abnormally high initial water contact angles (~110°), followed by a transient decay to lower contact angle values over a period of several minutes. These unusually high initial water contact angles are quite remarkable considering that the multilayer coating comprises only very hydrophilic polymers that are water-soluble in non-cross-linked forms and well-known for their ability to strongly interact with water molecules. Unlike conventional hydrophobic surfaces, these coatings have the distinct capacity to alter reversibly their surface structure in order to minimize their interfacial free energy with a surrounding medium. In addition, this new nanostructured multilayer coating can simultaneously present a very hydrophobic character to water droplets (close to a Teflon-like surface) and exhibit the capacity to absorb a substantial amount of molecularly dispersed, nonfreezing water *via* hydrogen-bonding interactions.[35−37] We refer to this unique combination of properties as "zwitter-wettability" and note that such behavior requires a specific combination of molecular and structural features that are readily created by controlling the processing parameters and materials used in the layer-by-layer nanoscale assembly process.

RESULTS

We previously reported that multifunctional thin film coatings composed of PVA and PAA could be layer-by-layer assembled under low pH conditions and subsequently stabilized to high pH by either postassembly thermal or chemical treatments.[34] We anticipated that the resultant hydrogel-like multilayers would be good candidates for preparing hydrophilic-type antifogging coatings with performance similar to coatings based on multilayers assembled from hydrophilic polysaccharides.[1] To screen these coatings and compare to other control surfaces, samples were conditioned at −20 °C and subsequently exposed to ambient lab conditions (22 ± 1 °C, 40 ± 10% RH).

As revealed in Figure 1b, under these conditions, hydrophilic glass (soda lime glass substrate treated with oxygen plasma using the procedure described previously[34]) and a 30-bilayer PVA/PAA multilayer film both exhibit initial high levels of frost formation followed by a slow clearing to a more transparent state. In the case of a hydrophobic fluorosilane-treated glass, the frosting persists for at least 30 s. Thus, under this particular challenge, both hydrophobic and hydrophilic glass as well as glass coated with a PVA/PAA multilayer thin film did not exhibit acceptable antifrost behavior.

To enhance the antifrost behavior of the PVA/PAA multilayer film, PEG molecules were reacted into the film as schematically illustrated in Figure 1a. The abundance of free hydroxyl and carboxylic acid groups in the as-assembled film allows for facile thermal and chemical modifications that enhance the stability of the film and provide additional functionality. As-assembled films (30 bilayers, 1610 ± 7 nm in thickness) were thermally cross-linked at 140 °C for 5 min to form ester linkages. Hydroxyl-terminated poly(ethylene glycol methyl ether) (M_w = 5000 g/mol) molecules were then reacted with the pH-stabilized films in phosphate buffer saline (PBS) solutions (pH ~7.4) using glutaraldehyde chemistry. The reaction was performed while the films are in a highly swollen state and after the PEG molecules have been allowed ample time (20 min) to diffuse throughout the film structure. Thus, the PEG molecules are dispersed throughout the entire film and not simply grafted onto the surface. Successful loading of the covalently attached PEG molecules throughout the multilayer film was confirmed by using a probe molecule as previously described[34] (for more details, see Supporting Information (Figure S2)). In addition, no significant change in thickness was observed after the PEG chemistry (thickness after reaction 1600 ± 29 nm), consistent with the conclusion that this reaction is not producing a dense grafted surface layer of PEG molecules. The final PEG-functionalized multilayer exhibited excellent optical quality and was uniform except at the edges of the glass slide, as is sometimes observed when glass slide size samples are coated with multilayers. Figure 1b shows the dramatic enhancement of antifrost behavior that results from this additional PEG chemistry. In contrast to the as-assembled multilayer and the control glass

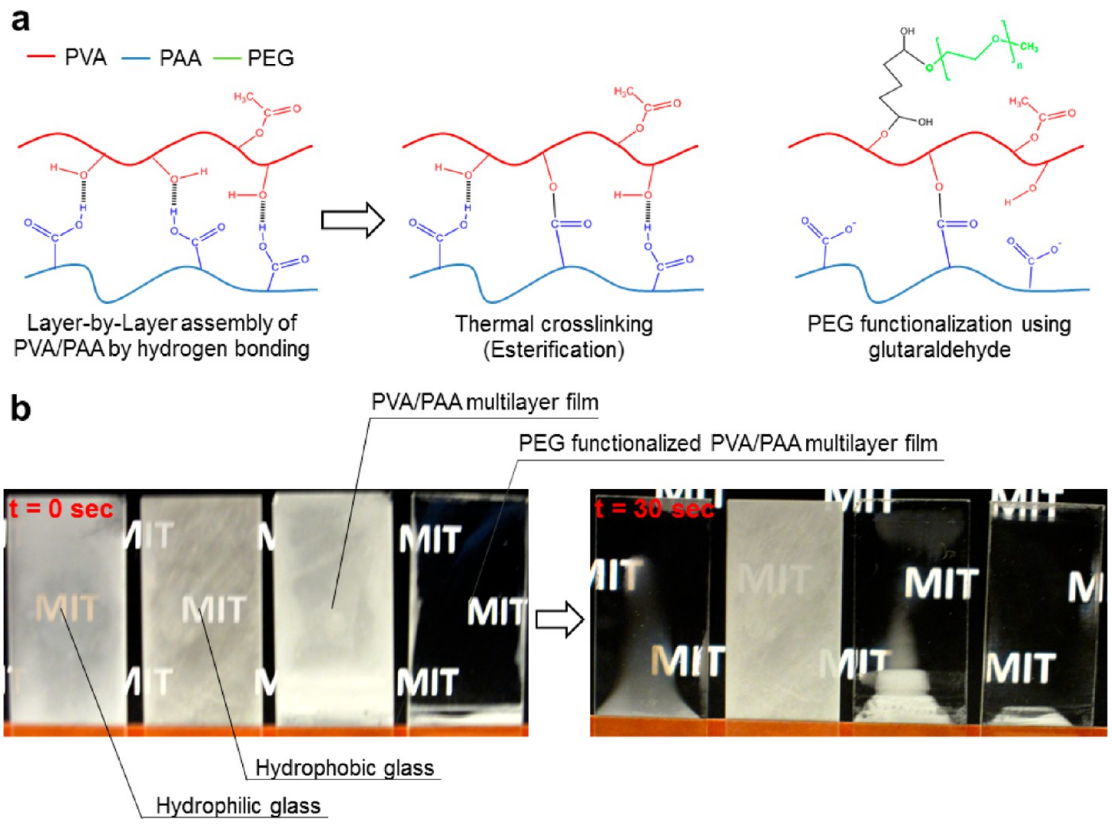

Figure 1. (a) Schematics showing the fabrication of the antifogging coating including reacting a thermally stabilized PVA/PAA multilayer film with poly(ethylene glycol methyl ether) (PEG) molecules. (b) Photographs taken immediately and 30 s after transfer to ambient lab conditions (22 ± 1 °C, 40 ± 10% RH) from a −20 °C freezer. Only the PEG-functionalized 30-bilayer PVA/PAA multilayer film resisted frost formation at the early and later stages of exposure. MIT logo in the figure was used with permission of Massachusetts Institute of Technology.

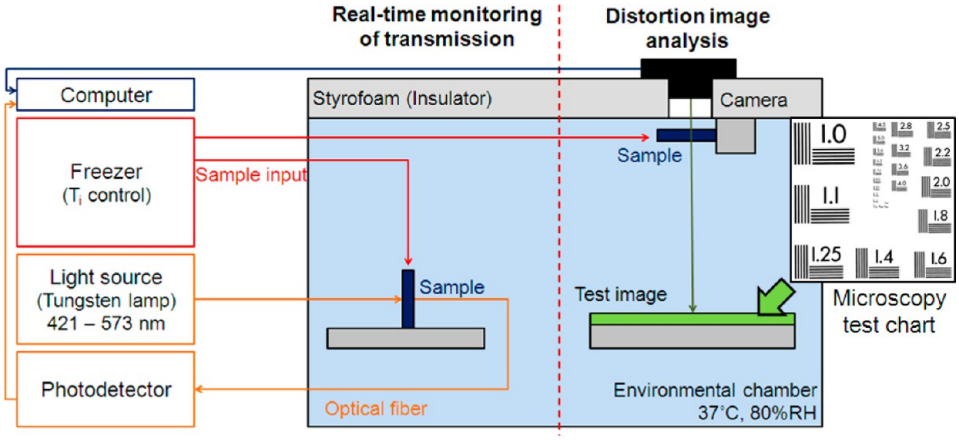

Figure 2. Experimental apparatus (real-time monitoring of transmission and distortion image analysis) used to quantify antifogging performance.

samples, the PEG-functionalized multilayer remains frost-free during the entire experiment.

To more completely assess the antifog/antifrost capability of this promising new coating system, real-time monitoring of both light transmission and image distortion was conducted under a variety of temperature/humidity profiles relevant to common fogging conditions, as shown in Figure 2. In order to provide context, PEG-functionalized multilayers were compared to a number of different control surfaces and coatings. A complete description of the testing apparatus and procedures can be found in the Methods section.

Figure 3 shows the normalized light transmission *versus* time of various coatings after exposure to 37 °C, 80% RH conditions with variation in T_i. Light transmission was normalized to the incident light intensity without any sample present. The level of image distortion observed from video images and the corresponding

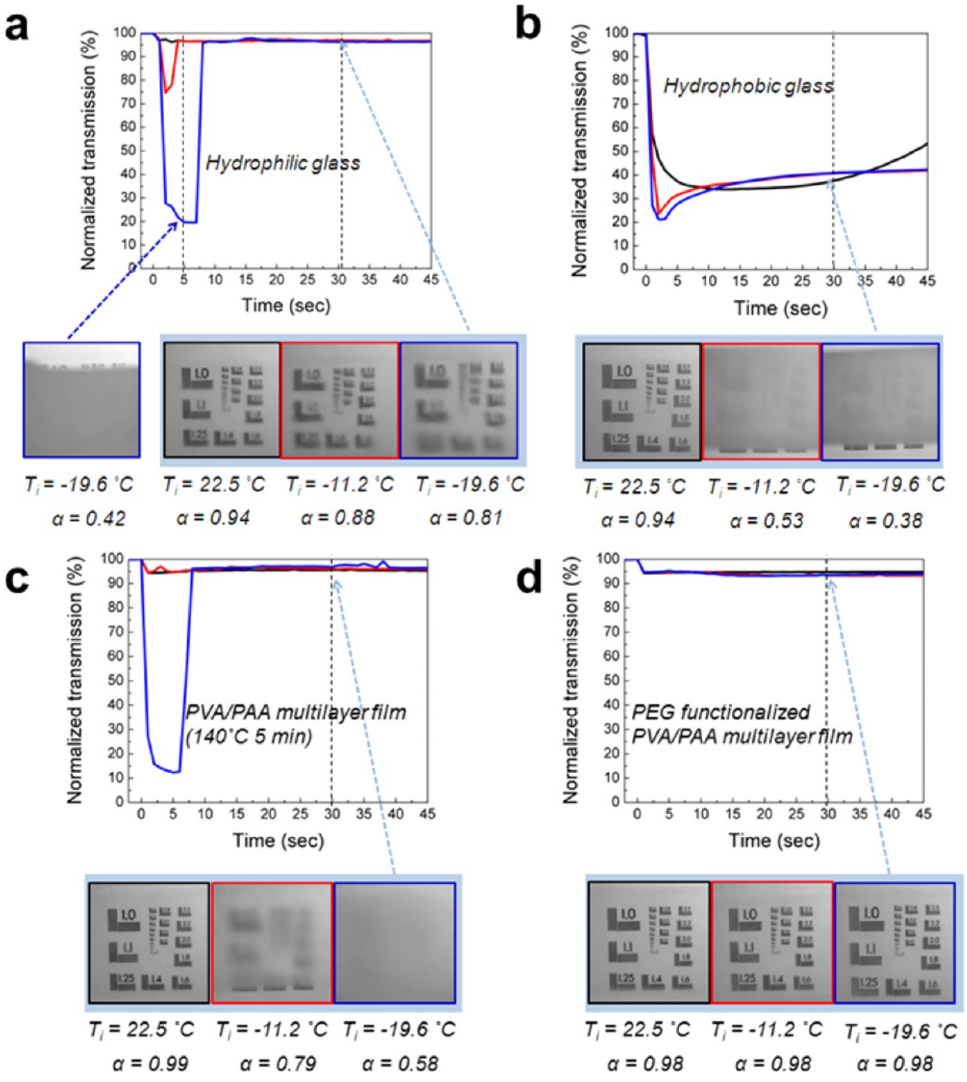

Figure 3. Normalized light transmission *versus* time of various coatings on glass after exposure to 37 °C, 80% RH conditions (black: T_i = 22.5 °C, red: T_i = −11.2 °C, blue: T_i = −19.6 °C). Light transmission was normalized to the incident light intensity averaged over the 421−573 nm range without any sample present. Below are images recorded through the sample at the indicated times and their corresponding α values. (a) Hydrophilic glass. (b) Hydrophobic glass. (c) PVA/PAA multilayer film (140 °C, 5 min). (d) PEG-functionalized PVA/PAA multilayer film.

correlation coefficient values (α) are also shown. The correlation coefficient (α) has a scale of 0 to 1, where 1 means no distortion and complete matching of the two images and 0 means no correlation among the images. Values of α above 0.95 correspond to essentially distortion-free behavior, while α below 0.5 corresponds to unacceptably poor visual clarity. Compared to the results shown in Figure 1b, these experiments were conducted in a more challenging environment for antifogging, *i.e.*, in more humid final conditions (37 °C, 80% RH) compared to ambient lab conditions (22 ± 1 °C, 40 ± 10% RH).

In the case of hydrophilic glass (water advancing contact angle of 8 ± 1°), high transmission and low image distortion levels are observed under the least challenging fogging conditions (T_i = 22.5 °C). This behavior is consistent with what has been reported[38] for hydrophilic surfaces. In sharp contrast however, under more aggressive fogging conditions, there is an initial sharp drop in transmission levels followed by a recovery to values above 90%. This early stage drop in transmission is due to frost formation facilitated by a conditioning temperature (T_i) that is below the freezing point of water. Of particular note is the fact that even though high transmission levels are recovered after the frost clears, images viewed through the glass samples are clearly distorted, as revealed by visual observation and by decreasing α values with lower temperature conditioning. Relatively high transmission levels are promoted in part by the presence of a low refractive index layer of water condensed on the surface ($n_{water} \approx 1.33$) compared to that of the glass substrate ($n_{glass} \approx 1.5$). Condensed water layers on both sides of the substrate enhance transmission levels *via* an antireflection mechanism, even though their presence also produces image distortion that would be undesirable for many optical applications. These very

hydrophilic surfaces also become less water wettable with aging under normal laboratory conditions. The net result as shown in the Supporting Information Figure S3a ("bare glass") is lower transmission levels and corresponding decreasing α values during fog testing. This is a well-known problem that occurs with highly energetic, very hydrophilic surfaces.[39]

Figure 3b shows the normalized light transmission and image distortion for the hydrophobic (advancing water contact angle of 112 ± 1°) fluorosilane-treated glass. Results reveal that not only does this hydrophobic coating exhibit significant distortion due to frosting and fogging but also the transmission values remain very low during the entire testing period. Clearly, typical hydrophobic surfaces are not well suited for handling an aggressive fogging challenge. In the case of a glass slide coated with the polymer poly(methyl methacrylate) (PMMA) (advancing water contact angle of 72 ± 2°), it was also found that low transmission values and high image distortion occurred during testing (Supporting Information Figure S3b).

When the PVA/PAA multilayer film was subjected to the same testing protocols (Figure 3c), it was found that samples conditioned at room temperature (T_i = 22.5 °C) maintained high transmission and low image distortion values during the entire testing period. However, decreasing T_i to −11.2 °C and further to −19.6 °C results in significant frost formation in the initial stages of the experiment and in corresponding reductions in α, to 0.79 and 0.58, respectively. Note also that after 10 s in the latter cases, the transmission levels are high even though the sample promotes significant image distortion. In sharp contrast to all of the samples tested, adding PEG segments to the PVA/PAA multilayer film produced a coating that maintained high normalized transmission levels (above 90%) and low image distortion (α values of 0.98) regardless of the initial conditioning temperature (Figure 3d). Thus, even under the most aggressive testing conditions, this coating effectively inhibits both frost formation and fogging.

On the basis of the full set of antifogging results for the various surfaces examined in this study, the following conclusions can be made. Hydrophilic glass surfaces can be effective at preventing fogging under mild conditions but are not able to prevent initial stage frost formation when samples are conditioned at temperatures below the freezing point of water. In addition, such surfaces can promote significant image distortion even after clearing of the frost. Commonly prepared hydrophobic surfaces, on the other hand, are unable to prevent fogging or frost formation under the conditions explored in this study. It is generally accepted that good antifog behavior is typically associated with surfaces that exhibit an advancing water droplet contact angle of less than 40°.[12,38] Hydrophobic surfaces are classically defined as having an initial advancing water droplet contact angle of 90° or higher and are generally not considered to be effective at preventing fog or frost formation. As will be discussed shortly, PVA/PAA multilayers, both as-prepared and PEG-functionalized, exhibit hydrophobic character when probed with water droplets (initial advancing contact angle ∼100° or higher). Clearly the excellent antifrost and antifogging capability of the PEG-functionalized multilayers is not consistent with conventional wisdom and warrants further clarification and understanding.

Wetting Properties of PEG-Functionalized PVA/PAA Multilayer Films. To investigate the origin of the excellent antifrost capabilities of PEG-functionalized PVA/PAA multilayers, time-dependent contact angle measurements were conducted for the three hydrophobic surfaces examined in this study: hydrophobic glass, as-prepared PVA/PAA multilayers, and PEG-functionalized PVA/PAA multilayers. As shown in Figure 4b, the surfaces of all of these coatings exhibited initial advancing water droplet contact angles of greater than 100°. In the case of the hydrophobic fluorosilane-treated glass (initial contact angle 112 ± 1°), the contact angle remains nearly constant with time. For the PVA/PAA multilayers and PEG-functionalized PVA/PAA multilayers, the initial contact angle (111 ± 3° for PVA/PAA multilayers and 117 ± 12° for PEG-functionalized PVA/PAA multilayers) drops slowly to much lower values over the course of the experiment, reaching about 70° for the PVA/PAA multilayer and about 50° for the PEG-functionalized PVA/PAA multilayer after 600 s. Not unexpectedly, the multilayer systems exhibit time-dependent behavior that is often attributed to transient surface reconstruction associated with a reorganization of hydrophilic functional groups to the surface in response to the water droplet.[40−45] Also note that the initial water contact angle of the PEG-functionalized PVA/PAA multilayer is essentially the same as that measured for the unmodified multilayer film. The observation of similar contact angles is consistent with the conclusion that a dense top layer of PEO is not grafted onto the surface.

In order to investigate this change in water contact angle more in depth, a drop shape analysis method was applied as reported previously.[41] Goniometry allows extraction of the droplet height (h), droplet width (r_b), and also its contact angle (θ) *versus* time as shown in Figure 4a. The spherical cap model was employed to determine the wetted surface area and the droplet volume. The initial droplet volume calculated using this model matched well with the actual water dispensed. The wetted surface area and droplet volume changes with time for the various samples were compared by using the equation given below.

$$S(t) = \pi r_b^2(t) \quad (1)$$

$$V(t) = \frac{\pi r_b^2(t)\, h(t)}{3} \frac{(2 + \cos\,\theta(t))}{(1 + \cos\,\theta(t))} \quad (2)$$

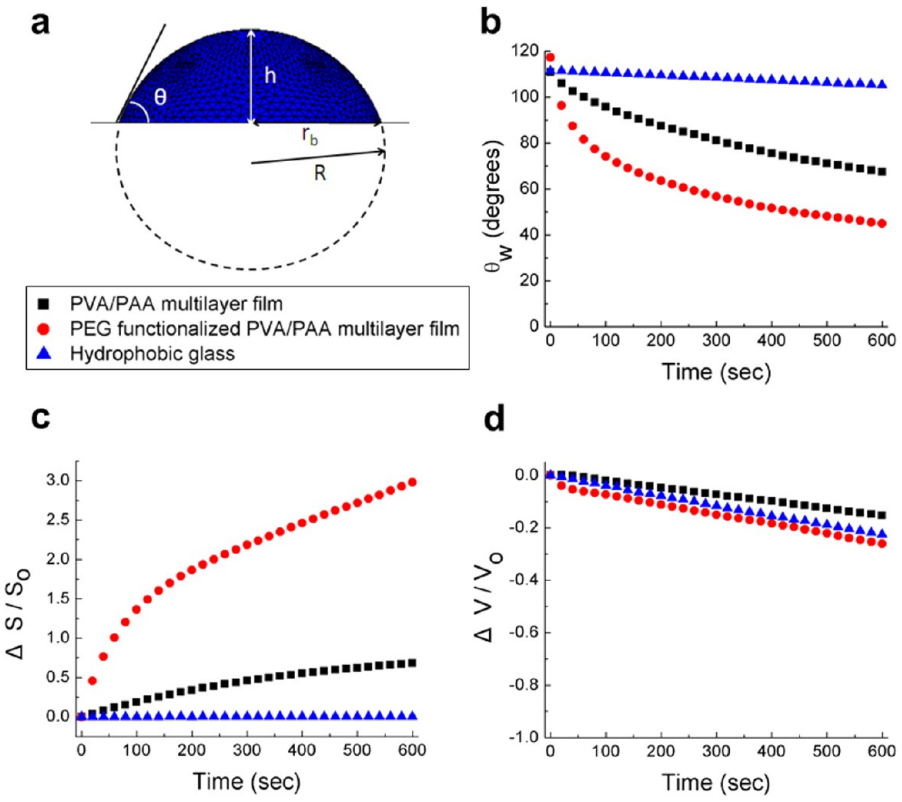

Figure 4. (a) Schematic representation of the spherical cap model used for the calculation of wetted surface area and droplet volume. (b) Water contact angle evolution over time (600 s) for three samples exhibiting hydrophobic behavior. (c) Wetted surface area evolution over time (600 s) for the three samples expressed as $\Delta S/S_o$ where $\Delta S = S - S_o$ and S_o is the initial wetted surface area at $t = 0$. (d) Water droplet volume evolution over time (600 s) for three samples expressed as $\Delta V/V_o$ where $\Delta V = V - V_o$ and V_o is the initial water droplet volume at $t = 0$. Filled symbols denote the average of three or more independent data points every 20 s.

where $S(t)$ and $V(t)$ define the wetted surface area and volume of the drop as a function of time, respectively. Figure 4c shows how the normalized wetted surface area changes with time for these samples. While the surface area for the hydrophobic fluorosilane-treated glass does not change with time, the data for the multilayer samples indicate an increase in the wetted surface area consistent with spreading of the water drops. For the PEG-functionalized PVA/PAA multilayer film, the wetted surface area increased nearly 300% over the 600 s time interval. However, from Figure 4d, where the normalized volume change with time is plotted, no significant difference in volume was observed (small, 10−20% decreases in volume can be anticipated due to evaporation of water from the droplets). From the multilayer results, it was concluded that the spreading of the water droplet dominates relative to the absorption of water into the film from the droplet over the 600 s of the experiment. Furthermore, PEG-functionalized PVA/PAA multilayer films exhibit a much faster evolving spreading of a water drop than the PVA/PAA multilayer films, suggesting that the surface reconstructs from a high initial to a lower final water contact angle more quickly for the PEG-functionalized PVA/PAA multilayer film.

It was unexpected for the PVA/PAA multilayer film and PEG-functionalized PVA/PAA multilayer film to exhibit such high values of the initial advancing water droplet contact angle (θ_w). Two main factors were considered as possible sources of this unusual behavior: (A) the presence of hydrophobic acetate groups in the partially hydrolyzed PVA polymer and (B) water droplet induced surface deformation at the three-phase contact line due to the intrinsically "soft" nature of the PVA/PAA multilayer film.

In the former case, it is to be recognized that the PVA used in the PVA/PAA multilayer films contains 11−16% acetate-bearing repeat units.[34] It is possible that these relatively hydrophobic moieties preferentially orient and become trapped at the film/air interface during the heating process used to thermally cross-link the film (140 °C for 5 min under vacuum). Similar abnormally high water contact angles have been reported before.[46−49] For example, nanocomposite poly(*N*-isopropylacrylamide) (PNIPA) films with clay network structures exhibited θ_w values in the range 100−131°. The authors attributed this behavior to the alignment of *N*-isopropyl groups of PNIPA chains at the gel−air interface. Consistent with the notion that the acetate groups are sufficiently hydrophobic to influence wettability, measurements of θ_w of poly(vinyl acetate) and partially hydrolyzed PVA with 11−16% acetate groups (films covalently bonded to a glass

substrate and heated at 140 °C for 5 min under vacuum) revealed advancing contact angles of 75 ± 2° and 75 ± 5°, respectively. In contrast, fully hydrolyzed PVA with 1−3% acetate groups exhibits a contact angle of 58 ± 1° after a similar heat treatment (see Supporting Information (Figure S4)).

With regard to the latter possibility, it was reported recently[50] that on thin soft substrates Young's law fails when there is substantial deformation near the three-phase contact line. Under such circumstances, the macroscopically observed contact angle increases and the substrate is effectively less wettable. As shown in the Supporting Information (Figure S5), PVA/PAA multilayer films that have been thermally cross-linked at 140 °C for 5 min show significant substrate deformation at the three-phase contact line after a hemispherical droplet of water is fully evaporated; more heavily cross-linked systems (140 °C, 10 and 30 min) do not show this behavior. On the basis of the previous predictions,[50] one would expect the contact angle to increase by a maximum of about 10° as a result of this effect. The additional enhancement in contact angle may be attributed to the chemical structure/mobility of the polymer matrix. It has been reported that the extent to which a gel surface may become hydrophobic by reorientation and conformational changes depends on the chemical structure of the polymer in the gel matrix and also on the mobility of the individual chain segments.[46] The effect of polymer mobility on the hydrophobicity of a hydrogel has been studied previously,[49] where a soft mobile gelatin gel with over 95% water content was found to have water contact angle in the range 90−120°.

It should be noted that others have suggested[51] that a rough surface could also contribute to the observation of very high values of θ_w. However, as reported previously,[34] PVA/PAA multilayer films have R_a roughness values of about 0.6 nm for ∼1.5 μm thick films, while the roughness of PEG-functionalized PVA/PAA multilayer films is about 1.8 nm. Thus an enhancement of θ_w due to high surface roughness was assumed to be negligible for both surfaces. We therefore conclude that the abnormally high initial values of θ_w observed on both PVA/PAA multilayer films and PEG-functionalized PVA/PAA multilayer films derive from the combined effects of the initially surface-enriched hydrophobic acetate moieties, the softness of the multilayer film, and the mobility of chain segments near the surface.

Condensation Experiments. One might expect that more hydrophobic surfaces inhibit the condensation of water by suppressing nucleation and that this effect might play a role in antifogging behavior.[52−55] To determine if the various surfaces investigated exhibited differences in water condensation during fogging conditions, the maximum amount of water condensed from moist air and steam was investigated. Various coatings (PVA/PAA multilayer film, PEG-functionalized PVA/PAA multilayer film, hydrophilic glass, and hydrophobic glass) were incubated at −20 °C for 1 h, and the mass change *versus* time was measured immediately after transfer to ambient lab conditions (22 ± 1 °C, 40 ± 10% RH). The maximum amount of water condensed was more or less the same (5−7 mg) for all of the coatings investigated regardless of their wetting properties except for the PVA/PAA multilayer film, which exhibited a larger amount of condensed water (9 mg) during the measured time period. Thus, no correlation between the amount of water condensed and antifrost/antifogging behavior was observed.

Effect of Elevated Temperature and Relative Humidity on Macroscopic Water Drop Profiles. The transient nature of the contact angle with time for the PVA/PAA-based multilayer coatings (Figure 4b) was previously attributed to surface functional group reorganizations in response to the presence of the probe water droplet. To examine if conditioning (for 1 h before water droplets added) the coatings in humid environments at higher temperatures would influence this effect, the evolution of macroscopic water drop profiles was examined in controlled environments at elevated temperature and higher humidity (37 °C, 80% RH). Both the PEG-functionalized and as-assembled PVA/PAA multilayers show faster decreases in contact angles with time and reach lower values of the contact angle when incubated and then probed in a higher humidity, higher temperature environment, as shown in Figure 5a, b, and c. However, even after conditioning in an environment that would be expected to render the coatings more hydrophilic due to reorganization of hydrophilic groups to the surface as reported previously by others,[43] the PEG-functionalized multilayer still exhibits an initial water droplet contact angle above 90° for the first 25 s of the experiment. In order to study this behavior in detail, another simple test was performed. A water drop was placed on a PEG-functionalized PVA/PAA multilayer film after being transferred to ambient lab conditions (22 ± 1 °C, 40 ± 10% RH) from a −20 °C freezer, as shown in Figure 5d. As revealed in this image, the coated section of the glass remains frost-free, indicating that molecularly condensed water has been effectively absorbed by the film. However, a water drop placed on top of this frost-free coating exhibits a water contact angle above 90°. Thus, this unusual surface simultaneously presents a very hydrophobic character, but also has the capacity to absorb a substantial amount of molecularly dispersed water. We refer to this unique combination of properties as "zwitter-wettability", as shown in Figure 5e.

Effect of Thermal Cross-Linking on Wetting Behavior. PVA/PAA multilayer films were thermally treated to varying extents to ascertain how increased cross-linking might influence wetting and antifrost behavior. Previously,

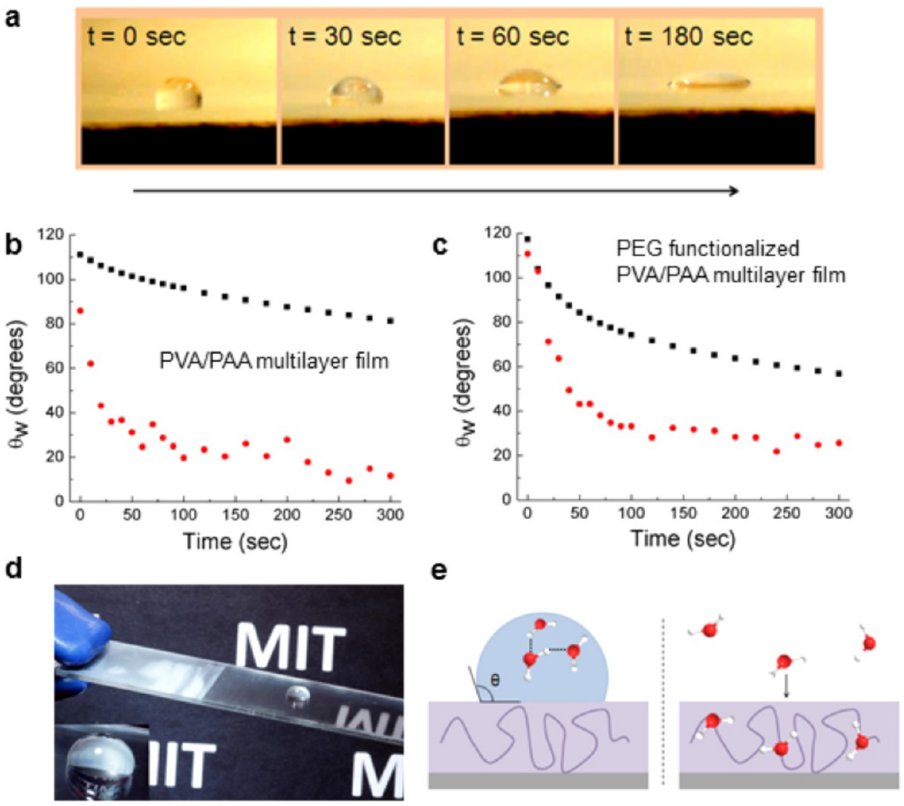

Figure 5. (a) Photographs of water drop profiles *versus* time on a PEG-functionalized PVA/PAA multilayer film in 37 °C, 80% RH conditions. (b) Water contact angle evolution over time (600 s) for a PVA/PAA multilayer film in ambient conditions and 37 °C, 80% RH conditions. (c) Water contact angle evolution over time (600 s) for a PEG-functionalized PVA/PAA multilayer film in ambient lab conditions (22 ± 1 °C, 40 ± 10% RH) and 37 °C, 80% RH conditions. (d) Photograph of a water drop placed on PEG-functionalized PVA/PAA multilayer film after being transferred to ambient lab conditions (22 ± 1 °C, 40 ± 10% RH) from −20 °C. Inset photograph shows the zoomed-in image of the water drop with a contact angle above 90°. Only the PEG-functionalized PVA/PAA multilayer coated part of the glass resist frost formation. (e) Schematic representation of zwitter-wettability. MIT logo in the figure was used with permission of Massachusetts Institute of Technology.

we have reported[34] that increasing the heating extent either by time or temperature alters the cross-link density of the multilayer film. Figure 6b shows how the swelling ratio (defined here as the ratio of the thickness of a film in contact with DI water to that of a dry film) changes with increase in heating time. For the 140 °C, 5 min treated sample, the swelling ratio was 3.6, and as the heating time increased from 5 to 30 min, a decrease in swelling ratio was observed: the corresponding values of swelling ratio were 2.9 and 2.3, respectively. Decreasing swelling ratios are consistent with an increase in cross-link density (Supporting Information Table S1). Figure 6a shows the transmission *versus* time plots of PVA/PAA multilayer films after exposure to 37 °C, 80% RH conditions for samples with the different thermal treatments. It is evident from the transmission experiment as well as the distortion analysis that increasing the cross-linking density is detrimental to the antifogging performance. Furthermore, a comparison of the transient water contact angle profiles of the PVA/PAA multilayer films with increasing cross-linking density (Figure 6c) revealed that the initial water contact angle of a PVA/PAA multilayer film decreases from 111 ± 3° to 77 ± 4°, and 70 ± 3°, with increasing cross-linking times. The abnormally high initial water contact angle (∼110°) shown for the 140 °C, 5 min treated PVA/PAA multilayer film is lost for the more heavily cross-linked systems and becomes closer to what was found for a poly(vinyl acetate)-coated glass (75 ± 1°). Thus, a more cross-linked film behaves as a more conventional hydrophilic coating. This result supports the hypothesis that the enhanced contact angle is due to the combined effects of a flexible surface enriched in hydrophobic acetate moieties and the softness of the multilayer film as mentioned earlier.

Effect of Overall Film Thickness and Type of Polymer Top Layer on Antifog/Antifrosting Behavior. The effects of bilayer number (or overall film thickness) and the type of polymer that was used in the last deposition step of the LbL assembly on antifog/antifrosting capabilities were investigated. The PVA/PAA multilayer films mentioned throughout this article are prepared by thermally cross-linking a 30 bilayer PVA/PAA multilayer film ($(PVA/PAA)_{30}$) on a glass substrate for 5 min at 140 °C; the 30 bilayer films are typically approximately ∼1.5 μm in overall film thickness. In order to explore the effect of overall film thickness, a six-bilayer PVA/PAA

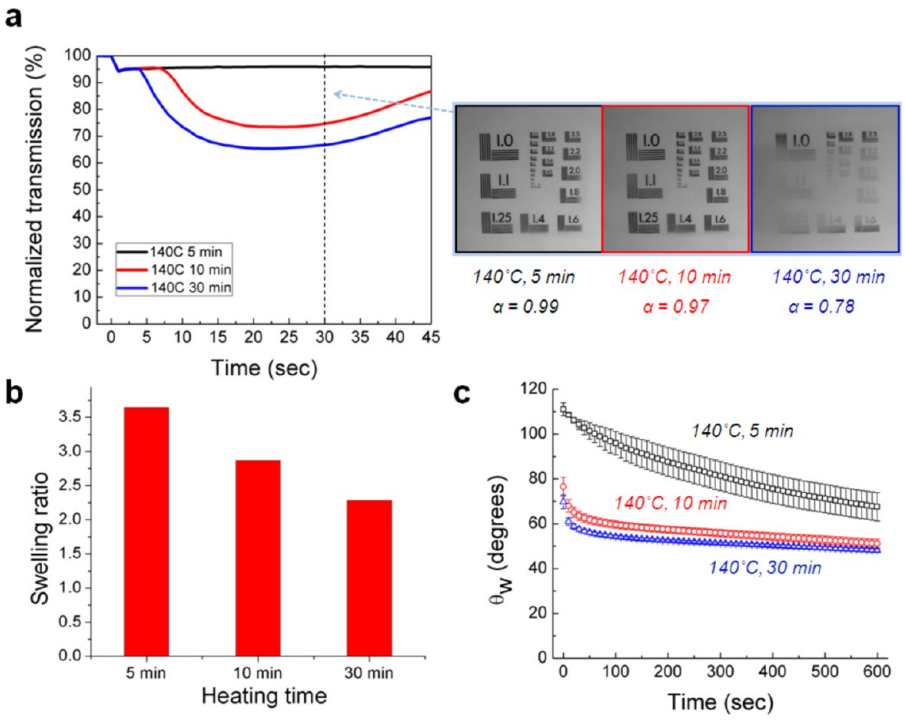

Figure 6. (a) Normalized transmission *versus* time after exposure to 37 °C, 80% RH conditions of PVA/PAA multilayer films thermally cross-linked with different heating times (5, 10, 30 min). Right photos are images recorded through the samples after 30 s and their corresponding α values. (b) Swelling ratio of PVA/PAA multilayer films with varying cross-linking treatments. (c) Water contact angle evolution over time (600 s) for PVA/PAA multilayer films in ambient conditions varying cross-linking treatments. Open symbols denote the average of three independent data points every 10 s.

multilayer film (~100 nm) and its PEG-functionalized counterpart were prepared. Transmission experiments and distortion image analysis on these thinner samples were performed, and the results (Supporting Information, Figure S7) show clearly that the antifog/antifrost performance of the six-bilayer films was inferior to the 30-bilayer films. Similar observations have been reported previously,[1] where a minimum critical thickness of the film was necessary to achieve acceptable antifogging performance.

The outermost layer effect was also investigated by ending the multilayer assembly with PVA: $(PVA/PAA)_{30.5}$. The noninteger value of Z indicates that the assembly process ends with the same polymer used to start the process; that is, the film is topped with the hydrogen-bonding acceptor PVA. As shown in the Supporting Information (Figure S8), regardless of which layer is on the top, functionalizing the PVA/PAA multilayer film with PEG results in excellent frost-resisting films.

Inhibition of Frost Formation. PVA/PAA multilayer films and PEG-functionalized PVA/PAA multilayer films are essentially soft coatings that have an abundance of hydrophilic functional groups that can absorb a substantial amount of water vapor from moist air. This property makes this system an extremely interesting platform for antifogging applications. However, it still remains a question why PEG-functionalized PVA/PAA multilayer films inhibit frost formation after incubation at very low temperatures and manage condensed water in such a way that minimizes image distortion. It has been reported[35,37,56] that water absorbed in certain polymer systems can exist in different states including nonfreezing (molecularly bound) and melting point depressed states. In this case, the water molecules are presumably molecularly dispersed as a result of strong polymer−water hydrogen-bonding interactions and hence are not capable of freezing at the usual temperature. One might expect that if this is the case in the PEG-functionalized PVA/PAA multilayer coatings, excess water on the surface could freeze, but water dispersed throughout the film would experience a depressed freezing point or none at all. In order to explore this hypothesis, samples were pre-exposed to different amounts of water prior to cooling (−20 °C) and subsequently tested under frost-forming conditions (Figure 7). Pretreatments before incubating in a freezer included (I) drying in ambient conditions, (II) immersion in DI water for 20 seconds followed by an exposure to compressed air just to remove the excess water layer on the top, and (III) immersion in DI water for 20 seconds followed by immediate transfer into the freezer. The observation of interference patterns after the treatment for sample II confirmed that the film absorbed a substantial amount of water prior to incubation in a freezer. As shown in Figure 7b, only sample III exhibited ice formation, with the surface ice eventually sliding across the film top surface. Sample II supports the idea that water existing in the multilayer

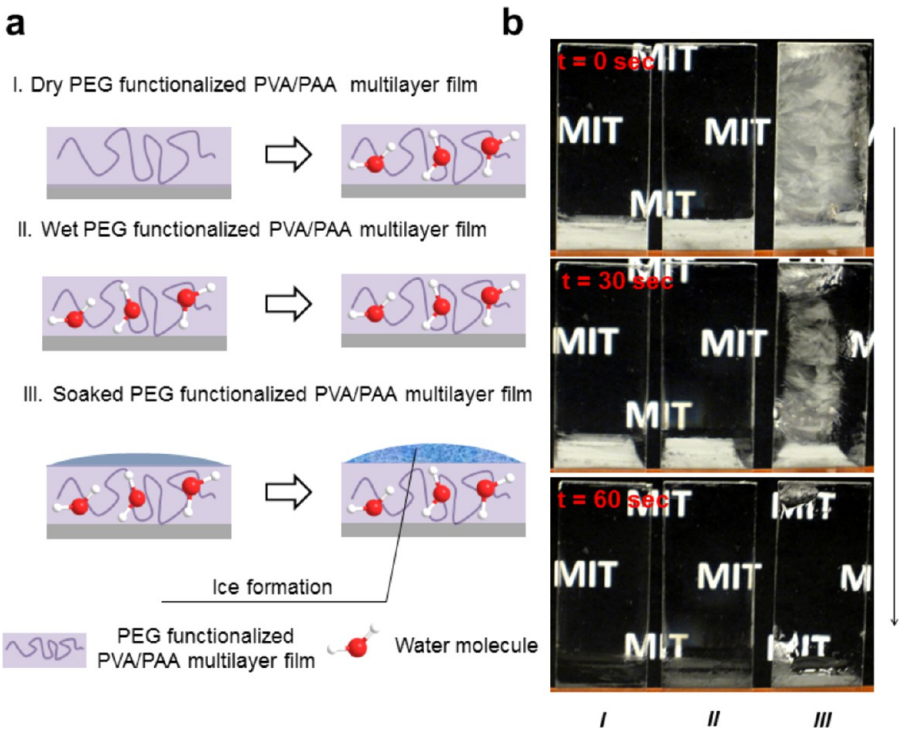

Figure 7. Frost formation experiment of PEG-functionalized PVA/PAA multilayer films with different water pretreatments. Samples were subjected to a −19.6 °C freezer for 1 h and exposed to ambient conditions (22 ± 1 °C, 40 ± 10% RH). (a) Schematic representation of how condensed water is presented after exposure to ambient conditions for differently pretreated PEG-functionalized PVA/PAA multilayer films: (I) Dry PEG-functionalized PVA/PAA multilayer film, (II) wet PEG-functionalized PVA/PAA multilayer film, (III) water-soaked PEG-functionalized PVA/PAA multilayer film. (b) Corresponding photos taken immediately and 30 and 60 s after exposure to ambient conditions for differently pretreated PEG-functionalized PVA/PAA multilayer films. Arrow indicates the direction of increase in time. MIT logo in the figure was used with permission of Massachusetts Institute of Technology.

film is nonfreezing and therefore imparts a resistance to frost formation even when a film is treated at temperatures below the normal freezing point of water.

DISCUSSION

Classically, a hydrophobic surface is defined as a surface that supports a water droplet advancing contact angle of 90° or higher. The PVA/PAA multilayer coatings, both as-prepared and PEG-functionalized, satisfy this simple definition. Both multilayer systems also exhibit a zwitter-wettable character, that is, the ability to rapidly absorb molecular water from the environment while simultaneously appearing hydrophobic when probed with water droplets. However, in the case of the PEG-functionalized multilayer, its special chemical and molecular architecture imparts a combination of physical properties that turn out to be uniquely suited for the prevention of frost formation and fogging. This combined zwitter-wettable and frost-resistant character requires a number of key molecular and structural features including (1) a surface enriched in hydrophobic moieties and (2) an abundance of available hydrophilic functional groups within the material that strongly hydrogen bond with water to produce a sufficient amount of nonfreezing water molecules. When these elements are in place, it is possible to create frost-resistant coatings that simultaneously exhibit both hydrophobic and hydrophilic characteristics.

The as-prepared PVA/PAA multilayer comes close to achieving all of the required elements, but only after adding PEG molecules does it become fully capable of resisting frost formation. The hydrophilic segments of both PEG[35] and PVA[56] are known to interact strongly with absorbed water molecules *via* hydrogen-bonding interactions to produce a nonfreezing bound state. Ultimately, however, it is the amount of nonfreezing water the material can accommodate that determines its effectiveness as an antifrost coating. The capacity of a material for absorbing a large amount of nonfreezing water is determined by its cross-link density (both physical and covalent), level of crystallinity, and level of competitive hydrogen bonding of the system.[35−37,56] In all of these cases, increases of the parameter will decrease the amount of nonfreezing water the system can accommodate. For the as-prepared multilayer, the molecularly blended hydrogen-bonded complex created by the nanoscale layer-by-layer assembly process ensures that crystallization of the PVA molecules will be limited or nonexistent. This same complexation, on the other hand, also reduces the amount of molecular interactions possible with water molecules (competitive hydrogen bonding). Likewise, the low

level of covalent cross-linking needed to stabilize the multilayer also decreases the nonfreezing water capacity of the system. Thus, the addition of PEG segments is needed to further increase the nonfreezing water capacity of the multilayer. The nanoscale layer-by-layer process for creating these PEG-containing multilayer films[57−59] makes it possible to optimize many of the key parameters responsible for the antifrost behavior. We therefore anticipate that further optimization of the structures of the polymers used and the assembly process could result in an as-prepared multilayer that exhibits antifrosting properties comparable to the PEG-functionalized system. It should also be noted that in the absence of nanoscale LbL assembly, cast films of the same PVA/PAA composition are rough and turbid (clearly not of optical quality), as shown in Figure S6. The enabling role of this nanoscale processing methodology is thus very apparent and critically important to the results presented in this paper.

The unusual hydrophobic nature of the multilayer is also a consequence of the structure and surface organization of the molecular complex formed by the layer-by-layer assembly process and subsequent chemical cross-linking. Previous reports of hydrophilic gels with unusually high advancing water droplet contact angles[46−49] conclude that this attribute is associated with the stable alignment of hydrophobic chain segments at the substrate surface. To achieve this alignment, the level of cross-linking and interchain molecular complexation (for multicomponent polymer systems) must be low enough to allow sufficient molecular mobility for the surface segments to achieve the required stable molecular conformations. As noted in this paper, increasing levels of cross-linking reduce the advancing contact angle to levels expected for a cross-linked homopolymer of partially hydrolyzed PVA (about 75°). Increasing levels of cross-linking and complexation also would be expected to decrease the compliance of the multilayer, thereby reducing the enhancement in contact angle due to the "softness effect" described in the Results section. Thus, to realize hydrophobic behavior that is observed even when a sample is incubated in a high humidity environment and preloaded with nonfreezing water, it is essential that the energetics favor surface alignment of the hydrophobic chain segments even when exposed to gas phase water. This was accomplished in the PVA/PAA multilayers by utilizing partially hydrolyzed PVA (provides the needed hydrophobic acetate groups), assembling under controlled pH conditions (controls the complexation process), and limiting the level of postassembly cross-linking. It should be noted that the hydrophobic character of this multilayer system may help to overcome a major problem with antifog coatings based on extremely hydrophilic, high surface energy materials, namely, a high susceptibility to fouling by low surface energy contaminates.[12,60] Additional work is required to confirm this possibility.

Finally, we note that the observation of zwitter-wettability is possible due to differences in the way water interacts with a surface when it is in a gas phase molecular state *versus* a droplet state. In the latter case, the liquid surface tension of water (γ_{LV}) dominates the initial interaction of the drop with the surface due to strong hydrogen bonding of water molecules within the water droplet. In contrast, molecularly dispersed water molecules in the atmosphere can directly diffuse into the multilayer film and interact with the abundant embedded hydrophilic groups. The net result is an ability to present simultaneously both hydrophobic character to water droplets and hydrophilic character to gas phase water molecules. This is possible, even after the thin film has absorbed a significant amount of water, as has been observed in certain polymer hydrogels.[46−49]

CONCLUSION

In summary, we show that zwitter-wettable surfaces, surfaces that simultaneously present a hydrophobic character and have the capacity to absorb a substantial amount of molecularly dispersed water, can be prepared using hydrogen-bonding-assisted LbL assembly of PVA and PAA. Real-time monitoring of transmission as well as distortion image analysis revealed that when PEG segments were reacted throughout the PVA/PAA multilayer, a coating was produced that maintained high normalized transmission levels and low image distortion regardless of the initial conditioning temperature. The net result was a coating system that effectively inhibited both frost formation and fogging.

Static water contact angle and swelling experiments indicated that the abnormally high initial advancing water contact angle of the multilayer platform (>100°) was attributed to the presence of surface-enriched hydrophobic acetate groups and the softness of the multilayer film. An abundance of hydrophilic functional groups within the material allows water droplets placed on a surface to spread by surface reconstruction and for molecularly dispersed water molecules to strongly hydrogen bond to produce nonfreezing water molecules. The addition of PEG to the PVA/PAA multilayer film provides an additional capacity to absorb nonfreezing water and an improvement in antifrost behavior.

METHODS

Materials. Asahiklin (AK225, Asahi Glass Company), poly(vinyl alcohol) (M_w = 131 000 g/mol, PDI = 1.50, 87−89% hydrolyzed, Sigma-Aldrich), poly(acrylic acid) (M_w = 225 000 g/mol, 20% aqueous solution, Sigma-Aldrich), glutaraldehyde solution (grade II, 25% in H_2O, Sigma-Aldrich), 2-butanone (MEK,

99+% ACS reagent, Sigma-Aldrich), poly(glycidyl methacrylate) (M_w = 25 000 g/mol, 10% solution in MEK, Polysciences), poly(methyl methacrylate) (M_w = 540 000 g/mol, Scientific Polymer Products), poly(ethylene glycol methyl ether) (M_w = 5000 g/mol, Sigma-Aldrich), and 1*H*,1*H*,2*H*,2*H*-perfluorodecyltrichlorosilane (Sigma-Aldrich) were used as received. Standard soda lime glass microscope slides and phosphate buffer saline were obtained from VWR. Deionized water (DI, 18.2 MΩ·cm, Milli-Q) was used in all aqueous polymer solutions and rinsing procedures.

Glass Substrate Pretreatment. The glass substrates were first degreased by sonication in a 4% (v/v) solution of Micro-90 (International Products Co.) for 15 min and subsequently sonicated twice in DI water for 15 min and dried with compressed air. They were then treated with oxygen plasma (PDC-32G, Harrick Scientific Products, Inc.) for 2 min at 150 mTorr. This glass is denoted here as hydrophilic glass and was used as the substrate for all the polymer coatings that were produced by layer-by-layer assembly. However, specifically for the PVA/PAA system, additional poly(glycidyl methacrylate) anchoring chemistry was included in order to covalently bond the first layer of PVA to the substrate, following the protocol described in our previous work.[34]

Coating Methodology. LbL assemblies of PVA and PAA were constructed using a Stratosequence VI spin dipper (Nanostrata Inc.) controlled using StratoSmart v6.2 software. LbL assembly employed dipping times of 10 min for the polymer solutions, followed by three rinses of 2, 1, and 1 min. The concentration of the polymer solutions was 1 mg/mL, and the pH of these solutions and the rinse water was adjusted to pH 2.0 with 0.1 M HCl or 0.1 M NaOH. The nomenclature for LbL films follows the following conventions: (hydrogen bonding acceptor/donor)$_Z$ where Z is the total number of bilayers deposited. The PVA/PAA multilayer film mentioned throughout this article is prepared by thermally cross-linking (PVA/PAA)$_{30}$ on a glass substrate for 5 min at 140 °C, unless other conditions are specified. The PEG-functionalized PVA/PAA multilayer film was prepared by immersing a PVA/PAA multilayer film in a 10 mg/mL PEG solution (pH 2.0) for 20 min. Then the sample was soaked at 30 °C in 0.13% (w/w) glutaraldehyde in PBS for 10 min, rinsed with DI water, and dried with compressed air. PMMA-coated glass was prepared by dissolving PMMA in Asahiklin at a concentration of 10 mg/mL. An approximately 150 nm thick coating was deposited onto a pretreated glass substrate by dip-coating for 1 h and heating the film for 1 h at ~60 °C to completely evaporate the solvent. Pretreated glass substrates were treated with 1*H*,1*H*,2*H*,2*H*-perfluorodecyltrichlorosilane by first placing them, along with a few drops of the reactive fluoroalkylsilane liquid, inside a Teflon canister under an inert nitrogen atmosphere and then sealing the canister and heating it overnight at 110 °C to result in hydrophobic fluorosilane-treated glass.[61]

Film Characterization. Dry film thicknesses were measured using a Tencor P16 surface profilometer with a 2 μm stylus tip, a 2 mg stylus force, and a scanning rate of 50 μm/s. Water contact angle measurements were performed using a Rame-Hart model 590 goniometer after vertically dispensing droplets of deionized water on various coatings. Water contact angles were measured as deionized water was supplied *via* a syringe into sessile droplets (drop volume ~10 μL). Measurements were taken at three different spots on each film, and the reported uncertainties are standard deviations associated with these contact angle values. The evolutions of water drop profiles in a controlled environment (37 °C, 80% RH) were measured by taking movies of the water drop inside the environmental chamber. Then, ImageJ software was used to fit the extracted images with the built-in angle tool. To determine the swelling ratio, a custom-built quartz cell was used in conjunction with a J.A. Woollam XLS-100 spectroscopic ellipsometer as described previously.[34] Data were collected between 400 and 1000 nm at a 70° incidence angle and analyzed with WVASE32 software. Condensation experiments were performed by preparing the samples on glass substrates of dimension 37.5 mm × 25.0 mm, equilibrating in the freezer set at −20 °C for 1 h, and measuring the mass change *versus* time immediately after transfer to ambient lab conditions using a digital scale balance (model Ag204, Mettler Toledo Instruments).

Antifogging Characterization. The quantitative antifogging performance on various coatings was evaluated in part by a customized setup in an environmental chamber as shown in Figure 2. Measurements were conducted by performing visible light transmission measurements (light source: tungsten lamp (421 nm −573 nm), detector: InstaSpec II, Oriel Instruments, monochromator: 125 mm spectrography/monochromator, model 77400, Oriel Instruments) on a sample in a controlled-humidity glovebox (environmental chamber, Electro-Tech Systems, Inc.). Optical fibers were used to measure the normalized transmission values inside the environmental chamber. Before measuring the real-time transmission behavior inside the controlled environment, the samples were first allowed to equilibrate for 1 h in a freezer set at a designated temperature (T_i) before being moved to the environmental chamber, which was maintained at 37 °C, 80% RH. Samples were transferred using a secondary container, and the exposure time was measured within 3 s after the sample was placed in the environmental chamber.

For the image distortion analysis, styrofoam was used as an insulator to inhibit the condensation of water vapor on the inner wall of the environmental chamber. A microscopy test chart was used for the test image. A reference video was taken with no sample between the camera and the test image. Exposure time was measured within 3 s after the sample was placed between the camera and the test image. Photos were extracted from the video at 5 and 30 s after exposure and referenced as target images. Distortion image analysis[62] was conducted by examining pixel intensity array subsets on two corresponding images (reference and target images) and extracting the deformation mapping function that relates the images, allowing a correlation coefficient to be obtained as shown in the Supporting Information (Figure S1b). Also, it should be noted that transmission measurement and image distortion analysis were conducted consecutively on the same sample with drying steps (in ambient conditions) in between.

Conflict of Interest: The authors declare no competing financial interest.

Supporting Information Available: Distortion image analysis, spectrofluorometry study of PEG-functionalized PVA/PAA multilayer film, real-time monitoring of transmission and its relevant distortion image analysis on bare glass and PMMA-coated glass, water contact angle measurements on various coatings, substrate deformation at the three-phase contact line of PVA/PAA multilayer film, estimation of cross-link density from swelling ratio, photograph of a film prepared from a solution of PVA and PAA, real-time monitoring of transmission and its relevant distortion image analysis of a PVA/PAA multilayer film and PEG-functionalized multilayer with six bilayers, photograph showing the top layer effect on antifog/antifrosting. This material is available free of charge *via* the Internet at http://pubs.acs.org.

Acknowledgment. We thank the Center for Materials Science and Engineering (CMSE), the Institute for Soldier Nanotechnologies (ISN), for use of their characterization facilities. We also thank J. Kleingartner for helpful discussions during the preparation of the manuscript and S. Srinivasan and K. Park for assistance with the contact angle measurements in the environmental chamber. This work was partially supported by a Samsung Scholarship and in part by the MRSEC Program of the National Science Foundation under award number DMR 0819762.

REFERENCES AND NOTES

1. Nuraje, N.; Asmatulu, R.; Cohen, R. E.; Rubner, M. F. Durable Antifog Films from Layer-by-Layer Molecularly Blended Hydrophilic Polysaccharides. *Langmuir* **2010**, *27*, 782–791.
2. Howarter, J. A.; Genson, K. L.; Youngblood, J. P. Wetting Behavior of Oleophobic Polymer Coatings Synthesized from Fluorosurfactant-Macromers. *ACS Appl. Mater. Interfaces* **2011**, *3*, 2022–2030.

3. Kaetsu, I.; Yoshida, M. New Coating Materials and Their Preparation by Radiation Polymerization. III. Antifogging Coating Composition. *J. Appl. Polym. Sci.* **1979**, *24*, 235–247.
4. Ueno, M.; Ugajin, Y.; Horie, K.; Nishimura, T. Antifogging Effect of Cellulose Films by Chemical Modification of the Surface Using Nonionic Fluorocarbon Surfactant. *J. Appl. Polym. Sci.* **1990**, *39*, 967–977.
5. Plasman, V.; Caulier, T.; Boulos, N. Polyglycerol Esters Demonstrate Superior Antifogging Properties for Films. *Plast. Addit. Compd.* **2005**, *7*, 30–33.
6. Xiong, J.; Das, S. N.; Kar, J. P.; Choi, J.-H.; Myoung, J.-M. A Multifunctional Nanoporous Layer Created on Glass through a Simple Alkali Corrosion Process. *J. Mater. Chem.* **2010**, *20*, 10246–10252.
7. Tricoli, A.; Righettoni, M.; Pratsinis, S. E. Anti-Fogging Nanofibrous SiO_2 and Nanostructured SiO_2−TiO_2 Films Made by Rapid Flame Deposition and *in Situ* Annealing. *Langmuir* **2009**, *25*, 12578–12584.
8. Shoji, A.; Fukushima, T.; Kumar, D. S.; Kashiwagi, K.; Yoshida, Y. Surface Modification of Plasma Polymerized Silicon Resin Films Produced at Different Gas Atmospheres. *J. Photopolym. Sci. Technol.* **2006**, *19*, 241–244.
9. Patel, P.; Choi, C. K.; Meng, D. D. Superhydrophilic Surfaces for Antifogging and Antifouling Microfluidic Devices. *J. Lab. Autom.* **2010**, *15*, 114–119.
10. Matsuda, A.; Matoda, T.; Kogure, T.; Tadanaga, K.; Minami, T.; Tatsumisago, M. Formation and Characterization of Titania Nanosheet-Precipitated Coatings *via* Sol−Gel Process with Hot Water Treatment under Vibration. *Chem. Mater.* **2005**, *17*, 749–757.
11. Lu, X.; Wang, Z.; Yang, X.; Xu, X.; Zhang, L.; Zhao, N.; Xu, J. Antifogging and Antireflective Silica film and Its Application on Solar Modules. *Surf. Coat. Technol.* **2011**, *206*, 1490–1494.
12. Howarter, J. A.; Youngblood, J. P. Self-Cleaning and Next Generation Anti-Fog Surfaces and Coatings. *Macromol. Rapid Commun.* **2008**, *29*, 455–466.
13. Dong, H.; Ye, P.; Zhong, M.; Pietrasik, J.; Drumright, R.; Matyjaszewski, K. Superhydrophilic Surfaces *via* Polymer−SiO_2 Nanocomposites. *Langmuir* **2010**, *26*, 15567–15573.
14. Du, X.; Liu, X.; Chen, H.; He, J. Facile Fabrication of Raspberry-like Composite Nanoparticles and their Application as Building Blocks for Constructing Superhydrophilic Coatings. *J. Phys. Chem. C* **2009**, *113*, 9063–9070.
15. Zorba, V.; Chen, X.; Mao, S. S. Superhydrophilic TiO_2 Surface without Photocatalytic Activation. *Appl. Phys. Lett.* **2010**, *96*, 093702–093704.
16. Zhang, L.; Qiao, Z.-A.; Zheng, M.; Huo, Q.; Sun, J. Rapid and Substrate-Independent Layer-by-Layer Fabrication of Antireflection- and Antifogging-Integrated Coatings. *J. Mater. Chem.* **2010**, *20*, 6125–6130.
17. Zhang, L.; Li, Y.; Sun, J.; Shen, J. Mechanically Stable Antireflection and Antifogging Coatings Fabricated by the Layer-by-Layer Deposition Process and Postcalcination. *Langmuir* **2008**, *24*, 10851–10857.
18. You, J.-H.; Lee, B.-I.; Lee, J.; Kim, H.; Byeon, S.-H. Superhydrophilic and Antireflective $La(OH)_3$/SiO_2-Nanorod/Nanosphere Films. *J. Colloid Interface Sci.* **2011**, *354*, 373–379.
19. Wang, J.-J.; Wang, D.-S.; Wang, J.; Zhao, W.-L.; Wang, C.-W. High Transmittance and Superhydrophilicity of Porous TiO_2/SiO_2 Bi-Layer Films without UV Irradiation. *Surf. Coat. Technol.* **2011**, *205*, 3596–3599.
20. Tahk, D.; Kim, T.-i.; Yoon, H.; Choi, M.; Shin, K.; Suh, K. Y. Fabrication of Antireflection and Antifogging Polymer Sheet by Partial Photopolymerization and Dry Etching. *Langmuir* **2010**, *26*, 2240–2243.
21. Cebeci, F. Ç.; Wu, Z.; Zhai, L.; Cohen, R. E.; Rubner, M. F. Nanoporosity-Driven Superhydrophilicity: A Means to Create Multifunctional Antifogging Coatings. *Langmuir* **2006**, *22*, 2856–2862.
22. Chevallier, P.; Turgeon, S. P.; Sarra-Bournet, C.; Turcotte, R. L.; Laroche, G. T. Characterization of Multilayer Anti-Fog Coatings. *ACS Appl. Mater. Interfaces* **2011**, *3*, 750–758.
23. Chien, D. M.; Viet, N. N.; Van, N. T. K.; Phong, N. T. P. Characteristics Modification of TiO_2 Thin Films by Doping with Silica and Alumina for Self-Cleaning Application. *J. Exp. Nanosci.* **2009**, *4*, 221–232.
24. Du, X.; He, J. Facile Fabrication of Hollow Mesoporous Silica Nanospheres for Superhydrophilic and Visible/Near-IR Antireflection Coatings. *Chem.—Eur. J.* **2011**, *17*, 8165–8174.
25. Gan, W. Y.; Lam, S. W.; Chiang, K.; Amal, R.; Zhao, H.; Brungs, M. P. Novel TiO_2 Thin Film with Non-UV Activated Superwetting and Antifogging Behaviours. *J. Mater. Chem.* **2007**, *17*, 952–954.
26. Han, J.; Dou, Y.; Wei, M.; Evans, D. G.; Duan, X. Antireflection/Antifogging Coatings Based on Nanoporous Films Derived from Layered Double Hydroxide. *Chem. Eng. J.* **2011**, *169*, 371–378.
27. Kwak, G.; Jung, S.; Yong, K. Multifunctional Transparent ZnO Nanorod Films. *Nanotechnology* **2011**, *22*, 115705.
28. Lam, S.; Soetanto, A.; Amal, R. Self-Cleaning Performance of Polycarbonate Surfaces Coated with Titania Nanoparticles. *J. Nanopart. Res.* **2009**, *11*, 1971–1979.
29. Law, W. S.; Lam, S. W.; Gan, W. Y.; Scott, J.; Amal, R. Effect of Film Thickness and Agglomerate Size on the Superwetting and Fog-Free Characteristics of TiO_2 Films. *Thin Solid Films* **2009**, *517*, 5425–5430.
30. Lee, D.; Rubner, M. F.; Cohen, R. E. All-Nanoparticle Thin-Film Coatings. *Nano Lett.* **2006**, *6*, 2305–2312.
31. Li, Y.; Zhang, J.; Zhu, S.; Dong, H.; Jia, F.; Wang, Z.; Sun, Z.; Zhang, L.; Li, Y.; Li, H.; *et al*. Biomimetic Surfaces for High-Performance Optics. *Adv. Mater.* **2009**, *21*, 4731–4734.
32. Liu, X.; Du, X.; He, J. Hierarchically Structured Porous Films of Silica Hollow Spheres *via* Layer-by-Layer Assembly and Their Superhydrophilic and Antifogging Properties. *ChemPhysChem* **2008**, *9*, 305–309.
33. Introzzi, L.; Fuentes-Alventosa, J. M.; Cozzolino, C. A.; Trabattoni, S.; Tavazzi, S.; Bianchi, C. L.; Schiraldi, A.; Piergiovanni, L.; Farris, S. "Wetting Enhancer" Pullulan Coating for Antifog Packaging Applications. *ACS Appl. Mater. Interfaces* **2012**, *4*, 3692–3700.
34. Lee, H.; Mensire, R.; Cohen, R. E.; Rubner, M. F. Strategies for Hydrogen Bonding Based Layer-by-Layer Assembly of Poly(vinyl alcohol) with Weak Polyacids. *Macromolecules* **2012**, *45*, 347–355.
35. Lin, C.; Gitsov, I. Synthesis and Physical Properties of Reactive Amphiphilic Hydrogels Based on Poly(*p*-chloromethylstyrene) and Poly(ethylene glycol): Effects of Composition and Molecular Architecture. *Macromolecules* **2010**, *43*, 3256–3267.
36. Qu, X.; Wirsén, A.; Albertsson, A. C. Novel pH-Sensitive Chitosan Hydrogels: Swelling Behavior and States of Water. *Polymer* **2000**, *41*, 4589–4598.
37. Ostrowska-Czubenko, J.; Gierszewska-Drużyńska, M. Effect of Ionic Crosslinking on the Water State in Hydrogel Chitosan Membranes. *Carbohydr. Polym.* **2009**, *77*, 590–598.
38. Briscoe, B. J.; Galvin, K. P. The Effect of Surface Fog on the Transmittance of Light. *Sol. Energy* **1991**, *46*, 191–197.
39. Engländer, T.; Wiegel, D.; Naji, L.; Arnold, K. Dehydration of Glass Surfaces Studied by Contact Angle Measurements. *J. Colloid Interface Sci.* **1996**, *179*, 635–636.
40. Wang, Y.; Dong, Q.; Wang, Y.; Wang, H.; Li, G.; Bai, R. Investigation on RAFT Polymerization of a Y-Shaped Amphiphilic Fluorinated Monomer and Anti-Fog and Oil-Repellent Properties of the Polymers. *Macromol. Rapid Commun.* **2010**, *31*, 1816–1821.
41. Farris, S.; Introzzi, L.; Biagioni, P.; Holz, T.; Schiraldi, A.; Piergiovanni, L. Wetting of Biopolymer Coatings: Contact Angle Kinetics and Image Analysis Investigation. *Langmuir* **2011**, *27*, 7563–7574.
42. Horinouchi, A.; Atarashi, H.; Fujii, Y.; Tanaka, K. Dynamics of Water-Induced Surface Reorganization in Poly(methyl methacrylate) Films. *Macromolecules* **2012**, *45*, 4638–4642.
43. Vaidya, A.; Chaudhury, M. K. Synthesis and Surface Properties of Environmentally Responsive Segmented Polyurethanes. *J. Colloid Interface Sci.* **2002**, *249*, 235–245.

44. Ruckenstein, E.; Gourisankar, S. V. Surface Restructuring of Polymeric Solids and Its Effect on the Stability of the Polymer—Water Interface. *J. Colloid Interface Sci.* **1986**, *109*, 557–566.
45. Crowe-Willoughby, J. A.; Genzer, J. Formation and Properties of Responsive Siloxane-Based Polymeric Surfaces with Tunable Surface Reconstruction Kinetics. *Adv. Funct. Mater.* **2009**, *19*, 460–469.
46. Holly, F. J.; Refojo, M. F. Wettability of Hydrogels I. Poly-(2-hydroxyethyl methacrylate). *J. Biomed. Mater. Res.* **1975**, *9*, 315–326.
47. Haraguchi, K.; Li, H.-J.; Okumura, N. Hydrogels with Hydrophobic Surfaces: Abnormally High Contact Angles for Water on PNIPA Nanocomposite Hydrogels. *Macromolecules* **2007**, *40*, 2299–2302.
48. Haraguchi, K.; Li, H.-J.; Song, L. Unusually High Hydrophobicity and Its Changes Observed on the Newly-Created Surfaces of PNIPA/Clay Nanocomposite Hydrogels. *J. Colloid Interface Sci.* **2008**, *326*, 41–50.
49. Yasuda, H.; Sharma, A. K.; Yasuda, T. Effect of Orientation and Mobility of Polymer Molecules at Surfaces on Contact Angle and Its Hysteresis. *J. Polym. Sci., Polym. Phys. Ed.* **1981**, *19*, 1285–1291.
50. Style, R. W.; Dufresne, E. R. Static Wetting on Deformable Substrates, from Liquids to Soft Solids. *Soft Matter* **2012**, *8*, 3177–3184.
51. Cassie, A. B. D.; Baxter, S. Wettability of Porous Surfaces. *Trans. Faraday Soc.* **1944**, *40*, 0546–0550.
52. Varanasi, K. K.; Hsu, M.; Bhate, N.; Yang, W.; Deng, T. Spatial Control in the Heterogeneous Nucleation of Water. *Appl. Phys. Lett.* **2009**, *95*, 094101.
53. Beysens, D. The Formation of Dew. *Atmos. Res.* **1995**, *39*, 215–237.
54. Koutsky, J. A.; Walton, A. G.; Baer, E. Heterogeneous Nucleation of Water Vapor on High and Low Energy Surfaces. *Surf. Sci.* **1965**, *3*, 165–174.
55. Moazed, K. L.; Hirth, J. P. On the Contact Angle in Heterogeneous Nucleation upon a Substrate. *Surf. Sci.* **1965**, *3*, 49–61.
56. Cha, W.-I.; Hyon, S.-H.; Ikada, Y. Microstructure of Poly(vinyl alcohol) Hydrogels Investigated with Differential Scanning Calorimetry. *Makromol. Chem.* **1993**, *194*, 2433–2441.
57. Kim, H.; Doh, J.; Irvine, D. J.; Cohen, R. E.; Hammond, P. T. Large Area Two-Dimensional B Cell Arrays for Sensing and Cell-Sorting Applications. *Biomacromolecules* **2004**, *5*, 822–827.
58. Salloum, D. S.; Schlenoff, J. B. Protein Adsorption Modalities on Polyelectrolyte Multilayers. *Biomacromolecules* **2004**, *5*, 1089–1096.
59. Cortez, C.; Quinn, J. F.; Hao, X.; Gudipati, C. S.; Stenzel, M. H.; Davis, T. P.; Caruso, F. Multilayer Buildup and Biofouling Characteristics of PSS-b-PEG Containing Films. *Langmuir* **2010**, *26*, 9720–9727.
60. Gemici, Z.; Schwachulla, P. I.; Williamson, E. H.; Rubner, M. F.; Cohen, R. E. Targeted Functionalization of Nanoparticle Thin Films *via* Capillary Condensation. *Nano Lett.* **2009**, *9*, 1064–1070.
61. Meuler, A. J.; Chhatre, S. S.; Nieves, A. R.; Mabry, J. M.; Cohen, R. E.; McKinley, G. H. Examination of Wettability and Surface Energy in Fluorodecyl POSS/Polymer Blends. *Soft Matter* **2011**, *7*, 10122–10134.
62. Chinga, G.; Syverud, K. Quantification of Paper Mass Distributions within Local Picking Areas. *Nord. Pulp Paper Res. J.* **2007**, *22*, 441–446.